Pergamon

Cement and Concrete Research 30 (2000) 923–930

CEMENT AND CONCRETE RESEARCH

Electrical properties of fluidified Portland cement mixes in the early stage of hydration

G. Levita[a,]*, A. Marchetti[a], G. Gallone[a], A. Princigallo[a], G.L. Guerrini[b]

[a]Department of Chemical Engineering, Industrial Chemistry and Materials Science, University of Pisa, Via Diotisalvi 2, 56126 Pisa, Italy
[b]CTG — Italcementi Group, Via Camozzi 124, Bergamo, Italy

Received 2 August 1999; accepted 10 April 2000

Abstract

The electrical conductivity and the dielectric constant of cement mixes have been studied in the initial stages of setting to correlate the time evolution of the electrical parameters with the chemical and microstructural modifications. The formulations, based on a mix of Portland cement and microsilica, were fluidified with various amounts of an acrylic polyelectrolite and had a w/c ratio of 0.24. Measurements were carried out at ambient temperature for times of up to 40 h, in the frequency interval 30 Hz–200 kHz. The conductivity showed a marked decrease correlated with the loss of connectivity of the macroscopic porosity (depercolation). The time to the drop of conductivity depended linearly on the concentration of superplasticizer whose retarding effect was clearly evidenced. A dielectric amplification phenomenon was observed which vanished after the porosity depercolated. The temperature profiles of mixtures with different concentrations of the superplasticizer were drawn and a simple model was developed to compute the specific thermal power as a function of time. A substantial coincidence was found, on the time axis, between depercolation and maximum rate of setting. Vicat tests were also carried out. © 2000 Elsevier Science Ltd. All rights reserved.

Keywords: Electrical properties; Silica fume; Superplasticizer; Retardation

1. Introduction

The chemical, physical and mechanical processes that turn water–cement mixes into stone-like solids are very complex; some details of such processes are yet to be clarified. Among the several techniques of investigation, those based on monitoring the electrical properties during the initial setting and in the subsequent hardening period appear to be very promising. The electrical monitoring is based on the assumption that in a system undergoing physical and chemical modifications, the electrical parameters reflect the change of nature, mobility, concentration and distribution of the charge carriers and of the dipolar species associated to such modifications. The electrical properties of cement mixtures change for months after their preparation and it has been shown that the amount of water and its interaction with the CSH environment deeply affect the dielectric response [1,2]. The electrical methods have advantages over other methods in terms of sensitivity and speed. Moreover, they can be operated in situ [1,3–13]. Recent developments of experimental techniques and of computational support now allow fast data acquisition and on-line data processing.

In spite of the potentialities of the electrical methods, progress in this field has been slow, mainly because of the poor comprehension of the phenomena underlying the electrical response of cementitious materials at the microscopic level. It has also been shown [14] that the electrical response of cements during maturation is a useful tool to evaluate the microstructure evolution of the material. Early studies by Tamás et al. [15] have shown that the time dependence of the electrical response of cement pastes is complex and influenced by a number of variables such as water content, temperature, clinker fineness, gypsum and admixture content. The conductograms (electrical conductivity vs. time plots) are thus very informative and can be regarded as the fingerprints of specific formulations and cure conditions.

The phenomena that accompany the sol to gel transition (setting), which occurs when water–cement mixes turns

---

* Corresponding author. Tel.: +39-050-511-201; fax: +39-050-511-266.

E-mail address: levita@ing.unipi.it (G. Levita).

0008-8846/00/$ – see front matter
PII: S0008-8846(00)00282-9

into an infinitely connected body, can also be appraised. Such studies lead to a more general comprehension of the evolution of the microstructure of the system and also yield information that can be incorporated in process and quality control protocols. Monitoring the properties of manufactured goods is nowadays an essential requirement in quality control regimes. Furthermore, the knowledge of the electrical parameters is necessary for the development of accelerated maturation processes by electromagnetic heating [16]. The growing application of cathodic protection to reinforced concrete structures also requires the knowledge and the control of the electrical properties of the cementitious binder [17].

Most of the papers in the literature deal with the electrical and dielectric properties of conventional cementitious systems [1,14,18–21]. Perez-Pena et al. [22] examined densified formulations treated at 500°C to produce materials to replace conventional ceramics in electrical applications. Gu et al. [9] studied, by means of impedance spectroscopy, the effect of silica fume on the evolution of the microstructure in densified cements. Moukwa et al. [6] studied the electrical properties of formulations with a 0.3 w/c ratio and fluidified with calcium naphthalene-sulfonates. Similar systems have been recently examined by Torrents et al. [23] at low frequencies.

In this paper, we examine the electrical properties of densified cement/microsilica mixtures characterized by a low water content. Good fluidity was obtained by means of a superfluidifier (an acrylic polyelectrolyte) In particular, the decline of conductivity associated with the sol–gel transition, the retarding effect induced by the superplasticizer and the correlation between electrical parameters and reactivity, appraised by measures of temperature rise, are considered. These formulations are of great interest for the development of high performance cement-based materials.

2. Experimental

2.1. Materials and methods

Mixes were based on a type I 52.5 R (European standard ENV 197/1) Portland cement (Italcementi). Additives were microsilica (Elkem 940) and an acrylic superplasticizer (Superflux 2000 AC from Axim Italia, in the following labeled *sp*). Formulations and main features of components are reported in Table 1. Cement and microsilica were dry-blended and the concentrated superplasticizer aqueous solution (30% solid) was diluted to the required level with tap water. Ingredients were then mixed in a high shear planetary mixer (~ 4 min) and the mixture poured into the cell which was gently vibrated to get rid of entrapped air.

Table 1
Mixture compositions

Component	Parts by weight
Cement, CEM I 52.5 ITC Rezzato (Blaine 4600 cm^2/g)	100
Microsilica, powder Elkem 940 U (BET 200,000 cm^2/g)	11.1
Acrylic superplasticizer (Superflux 2000 AC Axim Italia — 30% dry content)	0.6–3
Total water	24.4

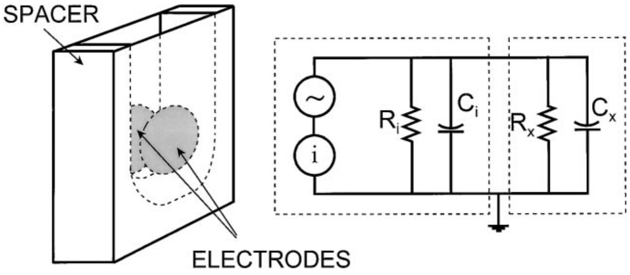

Fig. 1. Schematic of the cell and equivalent electric circuit of the bridge-cell assembly.

2.2. Electrical measurements

Measurements have been performed at ambient temperature with a GenRad 1693 RLC Digibridge in the frequency interval 30 Hz–200 kHz. The cell was in form of a plain capacitor made by two printed circuit boards on which circular electrodes (25-mm diameter) were obtained by etching. The boards constituted the cell walls and were kept in place by a U-shaped polyethylene spacer, 15-mm thick. The schematic of the cell and the equivalent circuit are in Fig. 1.

The real and imaginary components (ε' and ε_A'', respectively) of the complex dielectric constant, ε^* ($\varepsilon^* = \varepsilon' - i\varepsilon_A''$), and the electrical conductivity, σ, are given by Eqs. (1 and 2).

$$\varepsilon' = \frac{Y_X'' - Y_0''}{2\pi f C_0} + 1 \qquad (1)$$

$$\varepsilon_A'' = \varepsilon'' + \frac{\sigma}{2\pi f \varepsilon_0} = \frac{Y_X' - Y_0'}{2\pi f C_0} \qquad (2)$$

The apparent loss factor ε_A'' incorporates both the dipolar contribution, ε'', and the dissipation component, $\sigma/2\pi f\varepsilon_0$, originated by the flux of charge carriers. Y_X' and Y_0' are the real admittances of the system with and without the sample, respectively (Y_X'' and Y_0'' are the corresponding imaginary components); C_0 is the empty cell capacity; ε_0 (8.854×10^{-12} F/m) is the absolute dielectric constant of the free space; f is the frequency. The determination of C_0 (and minimization of stray effects) was made by filling the cell with cyclohexane ($\varepsilon' = 2.02$ and $\varepsilon'' = 0$ at room temperature).

The bridge, controlled by a microcomputer, was operated by a specifically developed software that allowed the temporized measure of admittances. The time taken to sweep the whole frequency range was about 30 s.

The electrical measurements started as soon as the cell, filled with the fresh paste, was electrically connected to the bridge. The first readings were taken about 5 min after the ingredients were mixed with a high shear stirrer.

2.3. Thermal measurements

Cylindrical casts of about 250 ml (diameter and eight about 6.8 cm) were placed in a cube of foamed polystyrene (edge 30 cm). The temperature at the center of the cast was measured with a thermocouple connected to a digital thermometer.

2.4. VICAT needle penetration tests

Penetration tests were made according to the EN 196, part III, test method. The needle diameter was 1.13 mm.

3. Results and discussion

Preliminary data showed that the electrical properties of all mixtures had major variations in the first 40 h; all measurements were therefore restricted to this length of time. In Fig. 2, values of ε' and ε_A'' are shown, as a function of frequency, for a mixture (sp/c = 0.02) at different levels of hydration. At low frequencies, both components of the dielectric constant had very high values ($\sim 10^8$) originated by double electric layers, located at the electrodes (electrode polarization) or at the surface of individual particles (interfacial polarization), that induced a dielectric amplification effect [24]. At high frequencies, the effect significantly reduced.

After 30 h, the dielectric constant, ε', of the paste, at 10^5 Hz, approached that of water, the most polar component of the mixes, whose ε' is at similar frequencies, around 80. Both the clinker and the portlandite are good insulators, $\sigma \sim 10^{-8}$ S/m, and have a low dielectric constant, $\varepsilon' \sim 5$ [25]; their contribution to the total polarization and conductivity of the paste is expected to be relevant only after the attainment of high levels of hydration, when the free water content is very low.

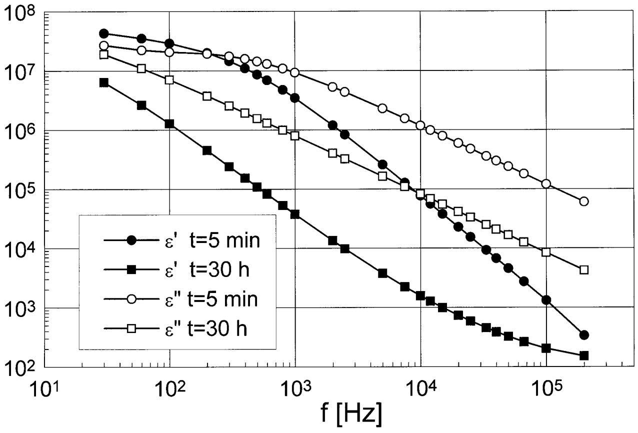

Fig. 2. Real and imaginary components of the dielectric constant vs. frequency for a mix with sp/c = 0.02, at two different times of maturation.

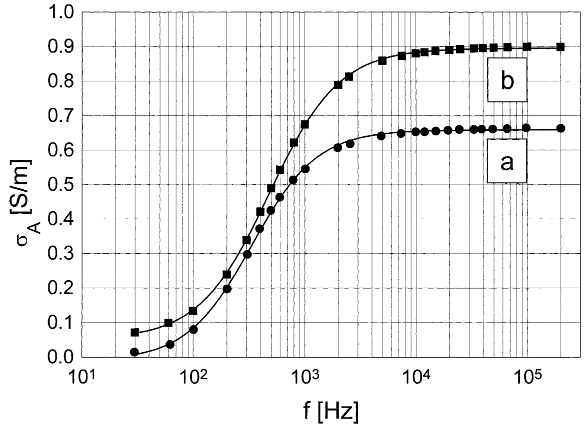

Fig. 3. Apparent conductivity vs. frequency for (a) a mix with sp/c = 0.015, 180 min after blending; (b) for the clear solution after leaching the cement powder with water (lines are the sigmoidal logistic fit).

The spectrum of ε_A'' showed in the central part of the explored frequency range a linear dependence on the logarithmic scale, Fig. 2, with a slope of about -1, due to the prevailing contribution of the electrical conductivity to the loss factor.

Both components of the complex dielectric constant decreased as the hydration progressed (Fig. 2). In principle, the decrease of the dielectric constant with time can be ascribed to three phenomena: (1) modification of the chemical nature of the constituents, (2) change of the relative amount of individual phases, and (3) variation of local topology. The first effect seems to be of little importance because the concentration of ionic components in the free water does not change significantly in time and the dielectric constants of clinker and of CSH are substantially similar [4]. Phenomena 2 and 3 are strictly related to each other. The hydration of cement is accompanied by a decrease of the free water content and an increase of the volume of the solid phase. The downward shift of the spectra of the dielectric constant has also been attributed to the thickening of layers in the CSH [5,18,24,26]. In general, factors that either increase the porosity (e.g., high w/c ratios) or decrease the thickness of the gel layers (e.g., short hydration times) increase the dielectric constant. The parallel decrease of pore size and the increase in gel layer thickness result in a decrease of the amplification effects [24]. The superplasticizer also influenced the dielectric constant due to the development of a finer porosity, as suggested in Ref. [26].

The electrical conductivity originates from the migration of charge carriers in the applied electric field. The presence of the electrode–fluid junctions gives rise to an additional polarization that limits the diffusive motion of the carriers. The double electric layers localized at the electrode–fluid interfaces are equivalent to capacitors in series with the sample; the net effect (diminution of conductivity) was

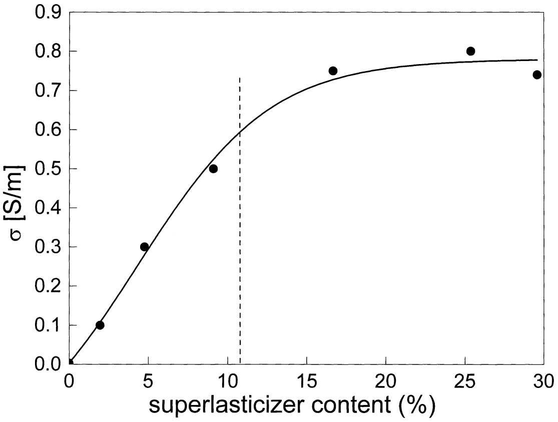

Fig. 4. DC conductivity of aqueous solutions of the superplasticizer vs. content of superplasticizer (concentrations used in the cement mixes are at the left of the dashed line).

evident at low frequencies and vanished progressively on increasing the frequency.

The apparent conductivity $\sigma_A(=\omega\varepsilon_0\varepsilon_A'')$ increased with frequency (Fig. 3a) and leveled out to a value assumed to be close to the real DC conductivity, σ, that would be measured at low frequency without polarization. All the σ values considered in this paper were taken at 150 kHz.

A different way to measure the conductivity, based on identifying the intersection points of the Y' vs. Y'' arcs in Nyquist's diagrams, is also frequently used [4,5,9,21,23,26,27]. Depending on composition, the initial conductivity of our mixtures varied approximately between 0.6 and 0.8 S/m. These relatively high values (that of drinkable waters is approximately in the range 0.04–0.1 S/m) almost entirely arose from the presence of Na^+, K^+, Ca^{2+}, OH^- and SO_4^{2-} ions in the pore water [28]. The conduction mechanism is electrolytic in nature and depends on ion concentration, ion mobility and temperature [19]. Tamás et al. [15] reported values of 1–2 S/m. Other researchers [22,28] found, for fluidified cement mixes, higher values (5–6 S/m), probably due to the greater quantity of water and, possibly, to the absence of microsilica in their formulations. Christensen et al. [28] verified that the presence of microsilica decreases the conductivity of the pore fluid probably because the pozzolanic character of the microsilica decreases the calcium hydroxide concentration.

Similar values of conductivity have been measured for the solution obtained leaching some cement powder in excess water for 30 min and allowing the dispersion to sediment. The dependence of the apparent conductivity of the solution from frequency was substantially similar to that of fresh cement pastes (Fig. 3b). This suggests that the polarization of the mixes essentially originated at the electrode–fluid junctions. The values of conductivity in Fig. 3b are similar to those found by Coverdale et al. (~ 1 S/m) [24] and by McCarter and Purygaud (~ 1.7 S/m) [3] for the conductivity of the pore fluid.

The contribution of the ionic superplasticizer to the conductivity of the mixes was also considered. The modifier is a polyelectrolyte and the conductivity of its aqueous solutions increased on increasing the superplasticizer content with a tendency to level off at high concentration (Fig. 4). In the examined cement formulations, the sp/c ratio varied from 0.006 to 0.3, which corresponded to sp/w ratios from 0.025 to 0.12. These values are in the linear range in Fig. 4 so that the initial conductivity of the cement mixes was expected to increase regularly on increasing the amount of superplasticizer. A clear dependence of the initial conductivity from the concentration of superplasticizer however was not found and a more complex behavior was found, as shown in Fig. 5 in which the variation with time of the conductivity of all the examined formulations is summarized.

In fact, several effects superimpose in the mixtures. The ionized molecules of the superplasticizer (anions) absorb on the surface of the granules so that the amount of mobile ions (macro-anions and cations) is less than the nominal value. Additionally, the superplasticizer deflocculates the cement paste causing an increase of the tortuosity of the ionic pathways; this effect would also bring about a diminution of conductivity. On the other hand, the conductivity of the aqueous phase increases with increasing polyelectrolyte content (Fig. 4). The net effect in the mixes is therefore hardly predictable, although a general tendency to a decrease was observed with increasing the additive concentration. This behavior, also noticed by Moukwa et al. [6], can also be explained by admitting that the superplasticizer adsorbed on the surface of the granules interferes with the normal process of ionic dissolution of some of the clinker constituents. Similar remarks were made by Torrents et al. [23].

It can also be noted that, at low superplasticizer contents, the internal structure of the paste (i.e., the dispersion of the smallest particles) is not easily reproducible. To confirm this, we prepared several formulations with the same low content of superplasticizer (sp/c = 0.008); the initial conductivity varied in the interval 0.6–0.7 S/m. The variability found for these formulations was therefore

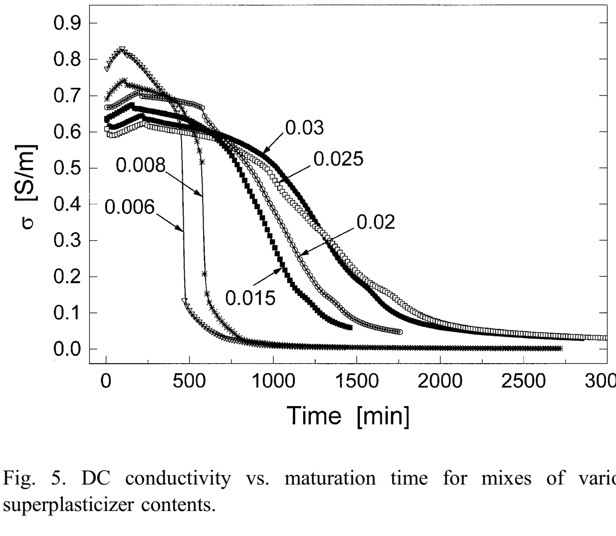

Fig. 5. DC conductivity vs. maturation time for mixes of various superplasticizer contents.

similar to that observed for the formulations with different superfluidifier contents. Thus, within our experimental resolution, the initial conductivity appeared to be a parameter of limited reliability.

Soon after mixing, the conductivity increased (Fig. 5), went trough a small maximum and then started to decrease monotonously; this effect has been noticed by different authors [22,29,30]. In general terms, the initial increase of conductivity can be attributed to various phenomena [6,19]: (1) increase of concentration of ions in the water solution; (2) increase of temperature caused by the exothermic reactions. The maximum has been attributed to the formation of a saturated or supersaturated solution of calcium hydroxide [31]. Tamás [20] studied the conductivity of pastes based on the pure constituents of Portland cements (C_3S, C_2S, C_3A and C_4AF) and noticed that the initial maximum of the conductivity was particularly evident for the C_3S and to a lesser extent for C_3A. We found that the position of this peak on the time axis was influenced by the amount of superplasticizer (Fig. 6).

The conductivity started to decrease markedly at the beginning of gel formation due to the reduction of the free water and to a diminution and segmentation of the capillary pores, which are the principal pathways for the ionic flow. A possible evaporation of the available water for high w/c ratios has also been proposed [4]. In our case, owing to the limited extent of free surface, this effect was marginal.

After the transition, the conductivity leveled out to about 10^{-2} S/m. The final conductivity was greater for the mixtures with higher superplasticizer contents. This can be attributed to the presence of not absorbed and ionized superplasticizer molecules in the pore solution. The time taken for the conductivity transition to complete was related to the amount of superplasticizer. We arbitrarily assumed that the sol–gel transition completed when the conductivity decreased to 0.1 S/m. The time taken to reach this value (sol–gel transition, t_{SG}) is shown in Fig. 6 as a function of the contents of superplasticizer. For sp/c ratio between 0.006 and 0.025, the relationship is nearly linear. The retarding effect leveled at high additive contents. The inhibiting effect of the superplasticizer is likely related to the level of superficial saturation of the finest particles, which substantially contribute to the extent of the solid–liquid interfaces.

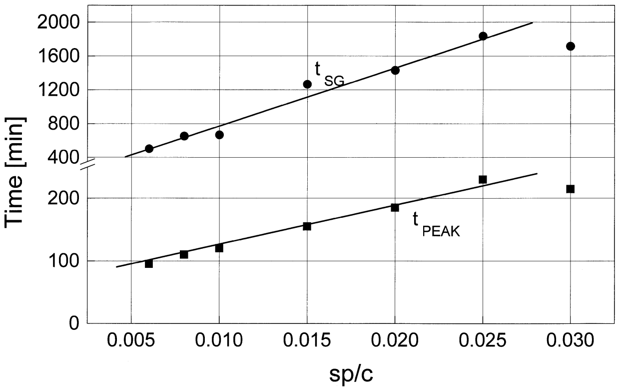

Fig. 6. Times at the first maximum and at the main transition vs. content of superplasticizer.

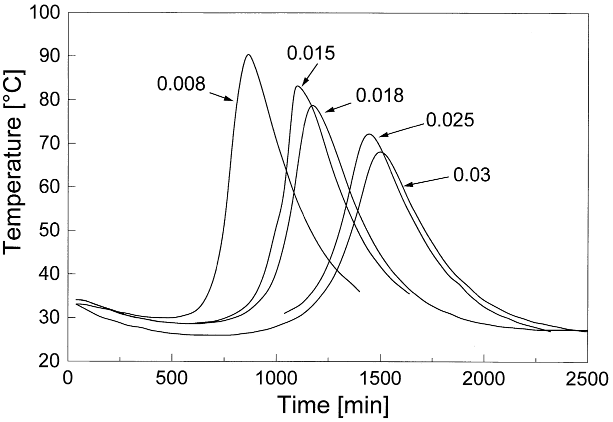

Fig. 7. Temperature vs. time for mixes with variable content of superplasticizer.

For a better comprehension of the setting process, it is useful to refer to the percolation theory. By this approach, it is easy to explain the various phenomena connected with the transition of the system from an open (connected) porosity to a closed (segmented) one. It is expected that such a transition will be accompanied by an abrupt decrease of conductivity because the charge carriers can only migrate through the capillary pore solution. The depercolation threshold (the porosity below which pores connecting the two electrodes through at least one continuos path no longer exists) is reached when the porosity falls approximately below 20%, a value almost independent of the particle size distribution [25]. The t_{SG} values we measured substantially agreed with the well-known data by Powers et al. [32] who established a correlation between the time necessary to segment the porosity and the w/c ratio.

The rise of temperature brought about by the hydration reactions was measured for all formulations in quasi-adiabatic conditions (Fig. 7). All curves were bell-shaped as a consequence of the imbalance between the rate at which heat is generated and the rate of dissipation. The former was larger at the beginning of setting, the latter predominated at later stages. At the very beginning, the temperature slightly decreased and started to markedly increase at the onset of the acceleration period. The maximum temperature was attained when the rate of heat evolution equated that of heat dissipation through the container walls.

The detrimental effect of the superplasticizer on the hydration process manifested in a shift toward longer times of the temperature peak that also widened. Because heat was generated in longer times, the maximum temperature decreased. As shown in Fig. 8, and according to Ref. [6], the maximum temperature and time to reach this maximum linearly depended on the contents of superplasticizer.

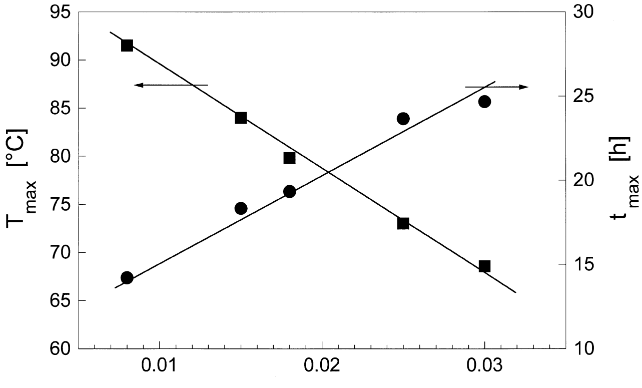

Fig. 8. Maximum temperature and time to maxima vs. content of superplasticizer.

It should be noted that the rate at which the temperature rose, decreased on adding the superplasticizer, whereas the rate of temperature decline was practically unaffected by composition. The maximum temperature occurred when the paste had already set.

The thermal power exchanged in the process, $P(t)$, was computed considering the heat generated by the hydration reactions and subsequently dissipated [see Eq. (3)]:

$$P(t) = C_P \frac{dT}{dt} + \frac{UA[T(t) - T_0]}{M} \tag{3}$$

where C_P is the specific heat of the set cement paste (~ 0.67 kcal/kg°C [33]); M is the weight of the sample (0.59 kg); A is the sample/container exchange surface (0.025 m^2); U is the thermal global exchange coefficient, substantially attributed to the container walls (~ 3.22 kcal/m^2 h°C); T_0 is the ambient temperature (~ 25°C); $T(t)$ is the sample temperature and t is the time (h). The experimental temperature profile and the computed thermal power are shown in Fig. 9 for one of the mixes. The values of the thermal power agreed with those of Moukwa et al. [6].

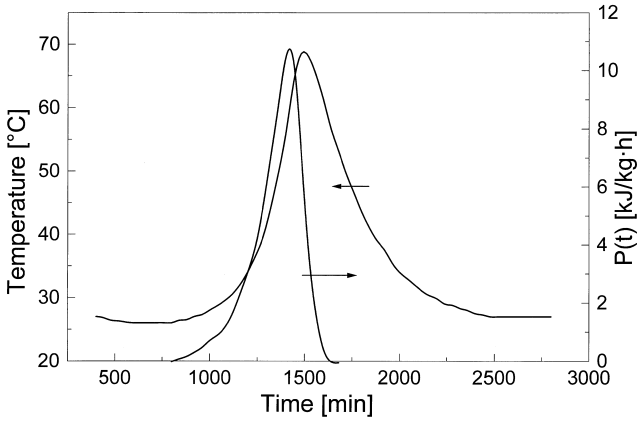

Fig. 9. Temperature and specific thermal power vs. time for a cement paste with sp/c = 0.03.

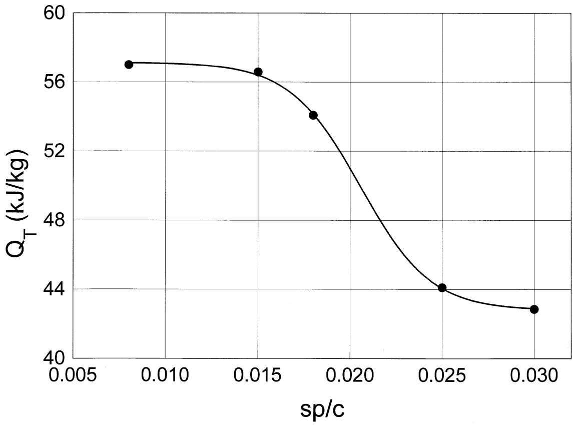

Fig. 10. Total heat vs. content of superplasticizer.

The total heat developed in the setting, Q_T, was calculated by integrating the thermal power [Eq. (4)]:

$$Q_T = \int_{t_1}^{t_2} P(t)\mathrm{d}t \tag{4}$$

were t_1 is the time at the initial temperature rise and t_2 the time when the sample was cooled to about the ambient temperature.

The total heat Q_T progressively decreased as the content of superplasticizer increased (Fig. 10). At low concentrations, there was no effect which, on the other hand, became evident for sp/c ratios above ~ 0.015; a saturation effect was observed above 0.025.

These observations can be related to those previously made about the initial conductivity of fluidified mixtures. It is known that the concentration of superplasticizers should be kept low both to limit costs and because no significant decrease in viscosity is produced above a threshold value. Both conductivity and thermal tests showed that the behavior of mixtures with sp/c ratios approximately below 0.015 differed from that of mixes richer in superplasticizer (the maximum recommended sp/c ratio, on the base of rheological tests, is for our system ~ 0.02).

The heat generated at time t is given by Eq. (5):

$$Q(t) = \int_{t_1}^{t} P(t)\mathrm{d}t \tag{5}$$

The ratio by Eq. (6):

$$X(t) = \frac{Q(t)}{Q_T} \tag{6}$$

($0 < X(t) < 1$ for $t_1 < t < t_2$) gives an idea of the completeness of the thermal process which is assumed to be completed at t_2 ($X(t)$ should not be confused with the advancement of the whole process of hydration which takes, in reality, much longer than t_2 to complete).

The sigmoidal $X(t)-t$ and $\sigma - t$ curves mirrored each other (Fig. 11). In particular, the position of the flex points of the two curves, i.e., the maximum rate of variation, coincided on the time axis. Some discrepancies were noticed for the formulations with very low sp/c ratios for which the collapse of conductivity anticipated the flex of the $X(t)$ curves. This effect and the different shape of the $\sigma - t$ curves of formulations with low superplasticizer content (Fig. 5) are likely related.

To evaluate the results of the electrical measurements against a more conventional technique, some penetration tests were made with the Vicat needle. The penetration test, although stingy in basic information, constitutes a good start for studies finalized to widen the potentialities of electrical methods. The Vicat test is very simple and its main limit is perhaps that of being sensitive only to the macroscopic behavior of the mixes. Another serious drawback we experimented, connected with the thixotropic nature of our formulations, was the fact that the needle was soon coated with a thick layer of cement so that the conditions of penetration, automatically operated, varied during the test.

In Fig. 12, the needle penetration is shown as a function of time for some formulations. The retarding action of the additive is evident. The penetration test is related, although in a complex way, to the resistance offered by the paste to the movement of a macroscopic probe. The conductivity test is somehow similar, with the important difference that the probe (ions) is very small. It is consequently reasonable that the transition from a freely flowing mixture to a clogged paste occurs in the Vicat test much earlier than for the conductivity test. The paste, already stiffened as not to allow the Vicat needle to penetrate, is still very porous so that ions can continue to easily migrate through it, even beyond the depercolation threshold. The electrical conductivity can therefore yield information also on the post-setting period.

It can also be noted that the electrical measurements can be conducted in the bulk of real formulations so that the data are readily applicable to large castings. Phenomena, such as bleeding, that modify the local conditions of castings could also be easily examined by reducing the size of the electrodes and placing them in the zone of interest.

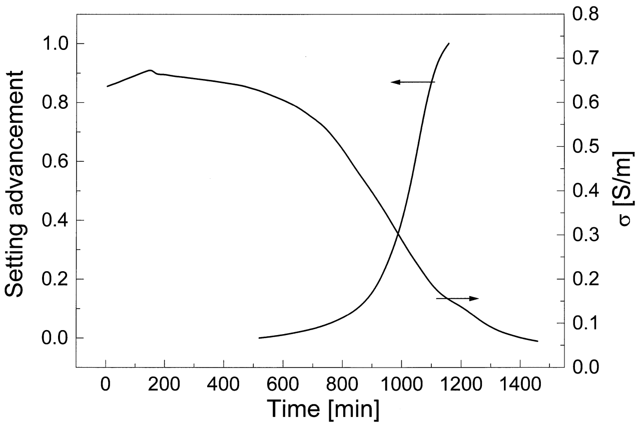

Fig. 11. Setting progress and DC conductivity vs. time for a cement paste with sp/c = 0.015.

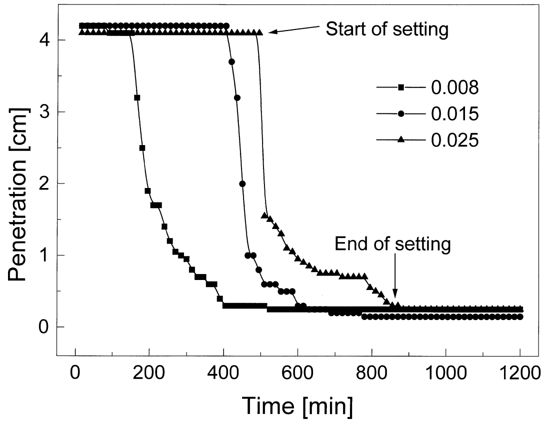

Fig. 12. Vicat penetration for mixes with different contents of superplasticizer.

4. Conclusions

The electrical conductivity and the dielectric constant of fluidified cement/microsilica pastes have been measured at $30-2 \times 10^5$ Hz at room temperature. An amplified response was obtained at low frequencies due to polarization effects, mainly occurring at the electrode–paste interface; the effect vanished above $\sim 10^4$ Hz. The initial DC conductivity, 0.6–0.8 S/m, of the various mixes was slightly less than that of the pore fluid ($\sim$ 0.9 S/m) and leveled off to about 10^{-2} S/m after about 30 h. The electrical parameters showed a transition, corresponding to the consolidation of the mix, attributed to the abrupt diminution of the amount of macroscopic capillary pores. The acrylic superplasticizer delayed the setting of formulations; the effect, linearly related to the superplasticizer content, was clearly evidenced by the electrical measurements. The shape of the transition was also influenced by the mix composition. The temperature of mixes was monitored and modeled to evaluate the rate of heat evolution and, consequently, of the advancement of the hydration reactions. A good match was found between electrical and thermal data. The electrically identified sol–gel transition occurred at longer times with respect to the loss of plasticity measured by the penetration tests. The reason is attributed to the small size of the probe in the former technique, which showed to be sensitive to the topochemical evolution at the microscopic level. The sensitivity and speed, connected with the possibility to perform remote measurements, confirm the electrical methods as a viable monitoring technique for the processing of high performances cement mixes. Finally, it can be noticed that by electrical means, it is possible to monitor fast processes such as the consolidation of rapid setting cements.

Acknowledgments

The authors gratefully acknowledge the financial support of the Progetto Strategico Microonde of the Italian CNR.

References

[1] P.R. Camp, S. Bilotta, Dielectric properties of portland cement paste as a function of time since mixing, J Appl Phys 66 (12) (1989) 6007–6013.

[2] P. Gu, J.J. Beaudoin, Dielectric behaviour of hardened cement paste systems, J Mater Sci Lett 15 (1996) 182–184.

[3] W.J. McCarter, P. Puyrigaud, Water content assessment of fresh concrete, Proc Inst Civ Eng Struct Build 110 (1995) 417–425.

[4] A. Berg, G.A. Nikalsson, K. Brantervik, Dielectric properties of cement mortar as a function of water content, J Appl Phys 71 (12) (1992) 5897–5903.

[5] G.M. Moss, B.J. Christensen, T.O. Mason, H.M. Jennings, Microstructural analysis of young cement pastes using impedance spectroscopy during pore solution exchange, Adv Cem Based Mater 4 (2) (1996) 68–75.

[6] M. Moukwa, M. Brodwin, S. Christo, J. Chang, S.P. Shah, The influence of the hydration process upon microwave properties of cements, Cem Concr Res 21 (1991) 863–872.

[7] I.L. Al-Qadi, O.A. Hazim, W. Su, S.M. Riad, Dielectric properties of portland cement concrete at low radio frequencies, J Mater Civ Eng 7 (3) (1995) 192–198.

[8] D.E. Macphee, D.C. Sinclair, S.L. Cormack, Development of an equivalent circuit model for cement pastes from microstructural considerations, J Am Ceram Soc 80 (11) (1997) 2876–2884.

[9] P. Gu, P. Xie, J.J. Beaudoin, R. Brousseau, A.C. Impedance spectroscopy (II): Microstructural characterization of hydrating cement–silica fume systems, Cem Concr Res 23 (1993) 157–168.

[10] U.B. Halabe, A. Sotoodehnia, K.R. Maser, E.A. Kausel, Modeling the electromagnetic properties of concrete, ACI Mater J 90 (6) (1993) 552–563.

[11] U.B. Halabe, K.R. Maser, E.A. Kausel, Condition assessment of reinforced concrete structure using electromagnetic waves, ACI Mater J 92 (5) (1995) 511–523.

[12] R. Zoughi, S.D. Gray, P.S. Nowak, Microwave nondestructive estimation of cement paste compressive strength, ACI Mater J 92 (1) (1995) 64–69.

[13] M.A. Taylor, K. Arulanandan, Relationships between electrical and physical properties of cement pastes, Cem Concr Res 4 (1974) 881–897.

[14] W.J. McCarter, P.N. Currant, The electrical response characteristics of setting cement paste, Mag Concr Res 36 (126) (1984) 42–49.

[15] F.D. Tamás, E. Farkas, M. Vörös, D.M. Roy, Low-frequency electrical conductivity of cement, clinker and clinker mineral pastes, Cem Concr Res 17 (2) (1987) 340.

[16] M. Leivo, Radio wave heating of concrete, Cem Concr Res 26 (5) (1996) 677–682.

[17] D. Buerchler, B. Elsener, H. Boehni, Electrical resistivity and dielectric properties of hardened cement paste and mortar, Mater Res Soc Symp Proc 411 (1996) 407–412.

[18] J. Ford, J.-H. Hwang, J.D. Shane, R.A. Olson, G.M. Moss, H.M. Mason, T.O. Mason, Dielectric amplification in cement pastes, Adv Cem Based Mater 5 (2) (1997) 41–48.

[19] H.W. Whittington, J. McCarter, M.C. Forde, The conduction of electricity through concrete, Mag Concr Res 33 (114) (1981) 48–60.

[20] D. Tamas, Electrical conductivity of cement paste, Cem Concr Res 12 (1982) 115–120.

[21] C.A. Scudieri, T.O. Mason, H.M. Jennings, Impedance spectra of hydrating cement pastes, J Mater Sci 26 (1991) 349–353.

[22] M. Perez-Pena, D.M. Roy, A.S. Bhalla, L.E. Cross, Dielectric properties of densified hardened cementious materials, Cem Concr Res 16 (1986) 952–965.

[23] J.M. Torrents, J. Roncero, R. Gettu, Utilization of impedance spectroscopy for studying the retarding effect of a superplasticizer on the setting of cement, Cem Concr Res 28 (9) (1998) 1325–1333.

[24] R.T. Coverdale, B.J. Christensen, T.O. Mason, H.M. Jennings, E.J. Garboczi, Interpretation of impedance spectroscopy of cement paste via computer modelling: Part II, J Mater Sci 29 (1994) 4984–4992.

[25] R.T. Coverdale, B.J. Christensen, H.M. Jennings, T.O. Mason, D.P. Garboczi, E.J. Garboczi, Interpretation of impedance spectroscopy of cement paste via computer modelling: Part I, J Mater Sci 30 (1995) 712–719.

[26] B.J. Christensen, R.T. Coverdale, R.A. Olson, S.J. Ford, E.J. Jennings, T.O. Mason, Impedance spectroscopy of hydrating cement-based materials: Measurements, interpretation, and application, J Am Ceram Soc 77 (11) (1994) 2789–2804.

[27] S.S. Yoon, H.C. Kim, R.M. Hill, The dielectric response of hydrating porous cement paste, J Phys D: Appl Phys 29 (1996) 869–875.

[28] B.J. Christensen, T.O. Mason, H.M. Jennings, Influence of silica fume on the early hydration of portland cements using impedance spectroscopy, J Am Ceram Soc 75 (4) (1992) 939–945.

[29] K. Olp, G. Otto, W.C. Chew, J.F. Young, Electromagnetic properties of mortar over broad frequency range and different curing time, J Mater Sci 26 (1991) 2978–2984.

[30] X.Z. Ding, X. Zhang, C.K. Ong, B.T. Tan, Study of dielectric and electrical properties of mortar in the early hydration period at microwave frequencies, J Mater Sci 31 (1996) 5339.

[31] F.M. Lea, The Chemistry of Cement and Concrete, Chap. 13, Edward Arnold, 1970.

[32] T.C. Powers, L.E. Copeland, H.M. Mann, Capillary continuity or discontinuity in cement pastes, J Portland Cem Assoc 1 (2) (1959) 38–48.

[33] W. Li, M.A. Ebadian, T.L. White, R.G. Grubbs, D. Foster, Heat and mass transfer in a contaminated porous concrete slab with variable dielectric properties, Int J Heat Mass Transfer 37 (1994) 1013–1027.